FLEROV LABORATORY OF NUCLEAR REACTIONS

In 2007, the FLNR scientific program on heavy-ion physics included experiments on the synthesis of heavy and exotic nuclei using ion beams of stable and radioactive isotopes and studies of nuclear reaction mechanisms, acceleration technology, heavy-ion interaction with matter, and applied research. These lines of research were represented in 19 laboratory topics and one all-institute project:

- Synthesis of new nuclei and study of the nuclear properties and heavy-ion reaction mechanisms (12 subtopics);
- Radiation effects and modification of materials, radioanalytical and radioisotopic investigations at the FLNR accelerators (5 subtopics);
- Development of the FLNR cyclotron complex for producing intense beams of accelerated ions of stable and radioactive isotopes (2 subtopics);
- Development and construction of an accelerator complex for producing radioactive ion beams (the DRIBs project).

In 2007, the operation time of the U400 and U400M FLNR cyclotrons was nearly 9000 h which is in accordance with the plan.

Synthesis of New Elements

During the recent years, essential progress in the experimental and theoretical investigations of the region of superheavy nuclei was achieved. The macro-microscopic (MM) nuclear model predicts a substantial enhancement of the stability of heavy nuclei when approaching the closed spherical shells at $Z = 114$ and $N = 184$. More recent microscopic Skyrme–Hartree–Fock–Bogoliubov (SHFB) or relativistic mean field (RMF) theories predict a large stabilizing effect of the neutron shell at $N = 184$ also, but suggest that the magic proton shell should be at higher proton numbers 120–126.

In the series of our previous experiments, 18 new nuclides with $Z = 112-118$ and their daughter isotopes were produced in the complete-fusion reactions of actinide target nuclei (^{238}U–^{249}Cf) with ^{48}Ca beams [1, 2]. The decay properties of these nuclei revealed a significant increase in their stability with approaching the hypothetical magic neutron number. The nuclides with the largest neutron and proton numbers $^{293}116$ ($N = 177$) and $^{294}118$ ($N = 176$) that were synthesized in the reactions with the heaviest isotopes ^{248}Cm and ^{249}Cf available for such experiments still possess 7–8 neutrons less than the predicted magic number. One can expect that the further increasing of neutron number in nuclei would result in further rise of their stability. However, the reactions with stable projectiles can lead to more neutron-rich isotopes of heavier elements only and require using of projectiles heavier than ^{48}Ca. Three reactions can be used for the synthesis of the isotopes of element 120 with the highest neutron number, in particular, $^{238}\mathrm{U} + {}^{64}\mathrm{Ni}$, $^{244}\mathrm{Pu} + {}^{58}\mathrm{Fe}$, or $^{248}\mathrm{Cm} + {}^{54}\mathrm{Cr}$, all of them leading to the same compound nucleus $^{302}120$.

According to the theory predictions, the maximum yield of evaporation residues in the reaction $^{244}\mathrm{Pu} + {}^{58}\mathrm{Fe}$ is expected for the $4n$-evaporation channel at $E_{\mathrm{lab}} = 330$ MeV. However, the calculated cross section value is far below the sensitivity of reasonable experiment ($\sigma_{4n} \sim 0.02$ pb). For estimating the survival probability of the compound nucleus during the de-excitation, the fission barriers calculated within the MM model were used ($Z_{\mathrm{magic}} = 114$). Correspondingly, the fission barriers of heavier nuclei become lower, that results in the gradual decrease in the survival probabilities and evaporation residue production cross sections. On the contrary, according to SHFB or RMF calculations, the fission barriers of nuclei, as well as their survival probabilities, should increase with approaching to $Z = 120$.

Furthermore, the use of the reactions of actinide target nuclei with heavier than ^{48}Ca projectiles (^{54}Ti, ^{58}Fe or ^{64}Ni) could reduce the fusion cross section. Therefore, different behaviour of complete-fusion reactions and the survival probability determined by the fission barrier of a heavy compound nucleus could noticeably influence the resulting production cross section of the

nuclei with $Z = 120$. The expected ER cross sections can vary within a wide range of 0.01–1 pb, that additionally stimulates the interest in the study of the reactions leading to the synthesis of element 120.

Due to the availability of the target material and projectile beam at the U400 cyclotron, we chose the reaction $^{244}\mathrm{Pu} + {}^{58}\mathrm{Fe}$. Irradiation of the ^{244}Pu target by ^{58}Fe projectiles was performed in January–March 2007. The decay chains that could be assigned to the isotopes of element 120 or its daughter nuclei were not observed during an irradiation with a beam dose of $7.1 \cdot 10^{18}$ of the 330-MeV ^{58}Fe projectiles. The sensitivity of the experiment corresponds to 0.4 pb for the detection of a single decay (1.1 pb is the upper cross-section limit). The low cross section together with that measured for the reaction $^{249}\mathrm{Cf}(^{48}\mathrm{Ca}, 3n)^{294}118$ in comparison with the corresponding values for $Z = 114$ and 116 nuclei could indicate receding from the stability region at $Z = 114$.

However, another very important reason for reducing the production cross section of the reaction $^{244}\mathrm{Pu}(^{58}\mathrm{Fe}, xn)$ could be stronger hindrance of the compound nucleus formation caused by the growth of the Coulomb repulsion force by about 30%, as compared with the reaction $^{244}\mathrm{Pu}(^{48}\mathrm{Ca}, xn)$. Further attempts to synthesize element 120 in the reaction $^{244}\mathrm{Pu} + {}^{58}\mathrm{Fe}$ require an increase in the sensitivity of the experiment. The more mass-asymmetric reaction $^{248}\mathrm{Cm} + {}^{54}\mathrm{Cr}$ is expected to be more preferable.

Chemistry of Superheavy Elements

Chemistry of Elements 112 and 114. In March–May 2007, a joint chemical experiment was performed together with radiochemical groups from PSI (Switzerland) and LLNL (USA). As compared with the previous 2006 experiment [3], the recoil transport and the detection system were improved. Transparency of the supporting target grid was increased to 85%. The speed of the transport gas was increased from 0.8 to 1.5 l/min. The transport PFA capillary was now heated up to 100 °C. The other equipment was the same as in the previous experiment. The first part of the experiment was dedicated to the confirmation of results obtained in 2006. A ^{242}Pu target (1.4 mg/cm^2), which was prepared on a thin (725 μg/cm^2) Ti foil, was irradiated during 3 weeks at the FLNR U400 cyclotron with $3.1 \cdot 10^{18}$ ^{48}Ca ions at an energy of 236 ± 3 MeV. The reaction $^{242}\mathrm{Pu}(^{48}\mathrm{Ca}, 3n) \rightarrow {}^{287}114 \rightarrow {}^{283}112$ was studied. During the experiment two atoms of ^{283}112 were adsorbed on the detector gold surface at temperatures -26 and -44 °C. Decay properties of ^{283}112 (E_α, half life time, TKE of fission fragments of the daughter isotope ^{279}110) confirmed the results of the previous «chemical» experiment [3] and the results obtained earlier at the DGFRS. Adsorption enthalpy describing 4 atoms observed in two «chemical» experiments was estimated to be 52 kJ/mol. As a result, we found that element 112 was very volatile and, unlike radon, revealed a metallic interaction with a gold surface. These adsorption characteristics establish element 112 to be a typical element of group 12. Due to the increased recoil delivery speed one α decay of $^{287}114$ ($T_{1/2} = 0.5$ s) was also detected. The energy $E_\alpha = 10.04$ MeV is in agreement with the α decay energy for ^{287}114 reported earlier at the DGFRS.

During the second part of the experiment the reaction $^{244}\mathrm{Pu}(^{48}\mathrm{Ca}, 3{-}4n) \rightarrow {}^{288-289}114 \rightarrow {}^{284-285}112$ was studied. Except for the target material (1.4 mg/cm^2 of ^{244}Pu), the experimental conditions and the setup were the same as in the first part of the experiment. After bombardment with the beam dose of $4.0 \cdot 10^{18}$ of ^{48}Ca two atoms of ^{288}114 and their daughter atoms ^{284}112 (SF) were observed. Again, the decay properties of those two isotopes were almost identical to the properties registered earlier at the DGFRS. The temperatures of adsorption of ^{287}114 and ^{288}114 determined in the experiment were found to be about -80 °C. This fact establishes for the first time that volatility of element 114 is close to that of heavy noble gases.

Experimental Study of the $^{136}\mathrm{Xe} + {}^{136}\mathrm{Xe}$ ***Reaction.*** The experiment aimed at the study of the symmetric reaction $^{136}\mathrm{Xe} + {}^{136}\mathrm{Xe} \rightarrow {}^{272}\mathrm{Hs}^*$ was performed in June–July 2007. The beam of $^{136}\mathrm{Xe}^{16+}$ with an intensity of about 2.5 eμA passed through a 4 μm Ti separating foil at the initial energy of 750 MeV. The target (99% ^{136}Xe enrichment) was kept at normal pressure. The target thickness was $3{\cdot}10^{18}$ Xe atoms (2.5 mg/cm^2). The beam energy in the center of the target chamber was 650 MeV. Another foil (13 μm Be) separated the target volume and the gas catcher chamber. Nuclear reaction products were stopped in the chamber, through which the transport gas (70% He, 20% Ar and 10% O_2) passed with a velocity of 0.9 l/min. The water vapour concentration in the gas was decreased to 1 ppm by passing the gas through a cartridge containing P_2O_5 as a drying agent before injecting it into the chamber. The reaction products were transported with the transport gas flowing through a 30 cm long quartz tube containing a quartz wool plug. The tube was heated to 650 °C and served as a filter for aerosol particles and provided an extended surface for the oxidation reaction of Os and Hs into their tetraoxides. The oxides were transported through a 8 m long perfluoroalkoxy (PFA) tube to the detection system. The detection system consisted of 8 pairs of silicon PIN-photodiodes 1×1 cm in the active area. The distance between the opposite PIN diodes was 1.5 mm. The detection system was kept at -50 °C according to the deposition temperature of HsO_4. The model experiment with the reaction $^{20}\mathrm{Ne} + {}^{156}\mathrm{Dy} \rightarrow {}^{176}\mathrm{Os}^*$ was performed to test the gas transport equipment and the detection system, to estimate the transport time of recoil nuclei and to select appropriate parameters for the main experiment. During the model experiment the gas transport time of 3 s was measured using ^{169}Os. Over a period of four weeks $3.6 \cdot 10^{17}$ ions were delivered to

the target. Observation of one decay corresponds to the cross section of $\sim$ 3 pb at given experimental conditions. Neither spontaneous fission nor alpha decay with energy of higher than 7 MeV was observed.

Nuclear Fission

The main task in 2007 was to carry out experiments aimed at understanding the dynamics of the process of formation and decay of superheavy nuclei. The main attention was paid to the study of influence of the entrance channel, evolution of the compound nucleus shape and competition between different exit channels (fission, quasi-fission). Measurements of the angular, mass and energy distributions of fission fragments allowed us to obtain information about the process of the compound nucleus fission as well as about the process of quasi-fission. The cross sections of these two processes were also measured. The experiment was carried out at the Flerov Laboratory of Nuclear Reactions in October 2007 with the use of the double-arm time-of-flight spectrometer CORSET. It was dedicated to the study of the processes of fusion–fission and quasi-fission in the reaction $^{36}\mathrm{S} + ^{238}\mathrm{U}$. Participants of the experiment were: the FLNR, Université Libre de Bruxelles (Brussels, Belgium), Dipartimento di Scienze Fisiche dell'Università di Napoli (Italy), Institut de Recherches Subatomiques (France), Laboratori Nazionale di Legnaro (Italy), Department of Physics of University Jyväskylä (Finland), and Institutions of the Republic of South Africa, iThemba LABS.

As a result, the absolute values of the capture, fusion–fission and quasi-fission cross sections for the reaction $^{36}\mathrm{S} + ^{238}\mathrm{U}$ were measured in an energy range 170–220 MeV with a step of about 10 MeV. A number of photovoltaic cells were installed at the angles θ = 130, 135, 140, 145, 150, 155, 160 and 165° to provide simultaneous measurements of the total quasi-elastic scattering cross section $\sigma_{\mathrm{qe}}(\theta)$. As the effective energy is expressed by $E_{\mathrm{eff}} = 2E/(1 + \mathrm{cosec}\,(\theta/2))$, this setup allows us to measure the energy dependence of the cross section more accurately and precisely define at what energy the measured σ_{ER} is peaked. Additionally, one can check if the measured total fission cross section is equivalent to that of the capture cross section. This technique was recently used in the reaction $^{86}\mathrm{Kr} + ^{208}\mathrm{Pb}$ at iThemba LABS (South Africa). The scheme of the experimental setup is presented in Fig. 1.

In 2007, the experiment dedicated to the study of the fragment mass distribution in the $^{238}\mathrm{U}(d, pf)$ reaction at intermediate energies was carried out. The experiment was done within the framework of the collaboration between the FLNR (JINR), LNS (Catania, Italy), the Accelerator Laboratory of the University in Jyväskylä (Finland), Dipartimento di Scienze Fisiche dell'Università di Napoli (Italy) and IN2P3 (France). We used the CORSET + DEMON + BaF + LCP setup to measure neutrons, γ-rays and light charged particles

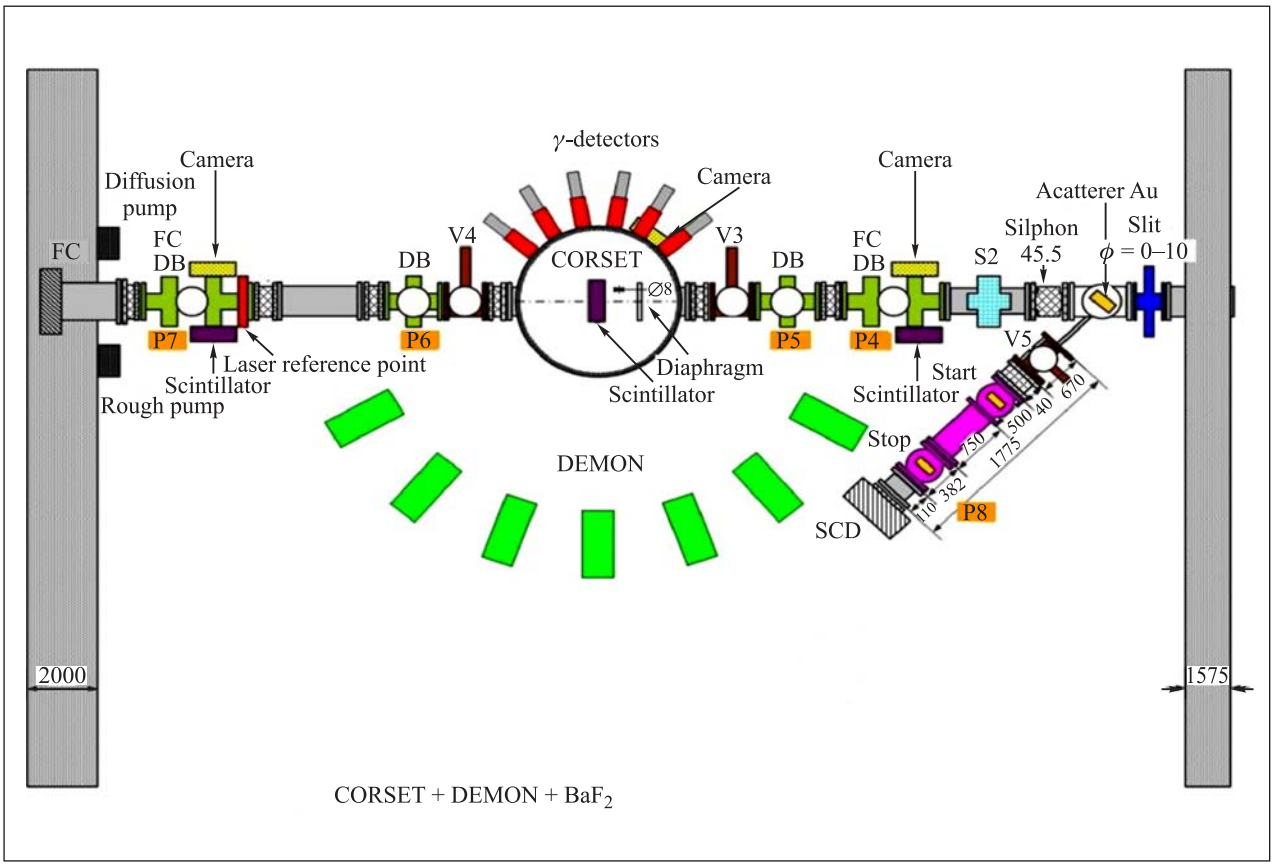

Fig. 1. The scheme of the experiment: DB — diagnostic block; FC — Faraday cup; P — pump; S — stirrer; V — valve

(protons) in coincidence with fission fragments in the reaction ^{238}U(d, pf) at $E_d = 125$ MeV. We studied the super asymmetric fission mode arising from the influence of the nuclear shells $N = 50$ and $Z = 28$ (^{78}Ni fission mode). At present the analysis of the obtained experimental data is underway.

The study of fission and evaporation residue formation cross sections was continued within the framework of the collaboration with the LNL (Legnaro, Italy). In 2007, the analysis of the data from the experiments carried out at LNL was finished and published in [4]. Mass–energy and angular distributions of fission fragments for the $^{48}\mathrm{Ca} + {}^{144,154}\mathrm{Sm} \to {}^{192,202}\mathrm{Pb}$, $^{40}\mathrm{Ca} + {}^{154}\mathrm{Sm} \to {}^{194}\mathrm{Pb}$ reactions were obtained. Fusion suppression and the presence of quasi-fission at energies near and below the Coulomb barrier were observed in the reactions with the deformed target ^{154}Sm. In the case of the spherical ^{144}Sm target no evidence of the quasi-fission manifestation was found. Quasi-fission cross sections were extracted from the data.

Separator VASSILISSA

In 2007, we continued experiments aimed at the study of decay properties of transfermium nuclei near the region of deformed neutron shells using reactions of ^{22}Ne with ^{244}Pu, ^{238}U at the recoil separator VASSILISSA equipped with a new detector system. It is a continuation of the program on the synthesis of new superheavy elements and the study of decay properties of isotopes of transfermium elements.

The isotopes of ^{255,256}No were produced with an intense (~ 2.0 pμA) ^{22}Ne beam impinging on the rotating ^{238}U target. The GABRIELA (**G**amma **A**lpha **B**eta **R**ecoil **I**nvestigations with the **EL**ectromagnetic **A**nalyser) setup was used in the measurements. During the experiment, calibration runs were regularly performed with the ^{164}Dy and ^{174}Yb targets to produce well-studied Rn and Th isotopes, in particular the well-known 181 μs isomeric state in ^{207}Rn to check the calibration of the electron detectors.

The analysis of these data is still in progress, but some modifications of the electronics and the focal plane chamber are being performed to increase the efficiency and sensitivity of GABRIELA in view of the next campaign of experiments. In particular, the number of electronic channels intended for β detection will be increased in order to measure efficiently β coincidences, and the thickness of the Al focal plane chamber will be reduced to increase low energy γ efficiency.

It was shown that rather high ($\sim 5\%$) transmission efficiency for slow evaporation residues could be achieved. This means that appropriate statistics for α–γ and α–β coincidences at the focal plane of the separator for neutron-rich Rf isotopes produced with the ^{22}Ne beam and ^{242}Pu target can be collected during one month of the beam time. This experiment is planned for the immediate future.

A systematic study of the spontaneous fission of transfermium nuclei is also planned using the complete fusion reactions $^{44}\mathrm{Ca} + {}^{208}\mathrm{Pb}$ and $^{22}\mathrm{Ne} + {}^{242}\mathrm{Pu}$. For this purpose a big neutron detector with 60 ^{3}He counters surrounding the focal plane semiconductor detector was designed. This detector allows us to measure neutron multiplicity of the spontaneous fission process of heavy transfermium nuclei.

In 2007, the project of modernization of the separator aimed at the study of the decay properties of isotopes of transfermium elements was started.

Two experiments were performed in collaboration with chemists. The first one was devoted to the study of chemical properties of elements 112 and 114 synthesized in the complete fusion reactions of ^{48}Ca with the ^{238}U, ^{242}Pu, ^{244}Pu targets.

The most important results obtained at the separator were published in [5–7].

Fragment Separator COMBAS

In 2007, experimental data obtained earlier in the reaction $^{22}\mathrm{Ne} + {}^{9}\mathrm{Be}$ at 40 A MeV at the in-flight separator COMBAS were analyzed. A hybrid model based on quantum molecular dynamics (QMD) and a statistical decay procedure were used for the description of experimental charge and isotopic velocity distributions of fragments emitted in the forward direction in the reaction studied. The analysis allows us to draw a conclusion about the domination of the mean field-like influence on the production of forward emitted fragments. The application of the model showed that the charge and velocity distributions could be reasonably well reproduced by the model simulation taking into account about 80% and 20% contributions of pure one-body and mean-field + two-body terms, respectively. Values of the fragment velocity exceeding the projectile velocity are not predicted by the model calculations. The work was performed in collaboration with a theoretical group from the H. Niewodniczanski Institute of Nuclear Physics (Krakow, Poland). The results of these simulations shall be published in the Acta Physica Polonica B journal.

A multi-detector system including 32 strip Si ΔE detectors and CsI(Tl) E detectors for correlation experiments at the in-flight separator COMBAS was commissioned. Thick coaxial Si(Li) drift detectors were used for the detection of long-range light particles. Detection of monochromatic radioactive ^{6}He and $^{7-9}$Li beams with an energy from 150 to 300 MeV shows that Si(Li) coaxial detectors allow the energy resolution in a range from 0.5 to 0.7%. It is better than the resolution of CsI(Tl) detectors (1–1.5%). A multichannel electronics system satisfying the requirements of high-resolution spectroscopy measurements was designed and commissioned.

In our previous experiments devoted to the study of spontaneous fission of ^{252}Cf we found multiple indications of unusual, at least ternary, decay channel called the collinear cluster tripartition (CCT). For better understanding of the physics of the effect we planned to investigate different fissile systems at different excitation energies of up to the threshold of the nuclear shell survival. One of the chosen reactions was $^{235}\mathrm{U}\,(n_{\mathrm{th}}, f)$.

The experiment was performed at the beam of thermal neutrons of the IBR-2 reactor of the Frank Laboratory of Neutron Physics with the help of the double arm TOF-E (time-of-flight vs energy) miniFOBOS spectrometer. The involved detectors let us calculate both pre- and post-neutron fragment masses, the velocity (momentum) vector, the range of the fragment in gas of the ionization chamber in each spectrometer arm.

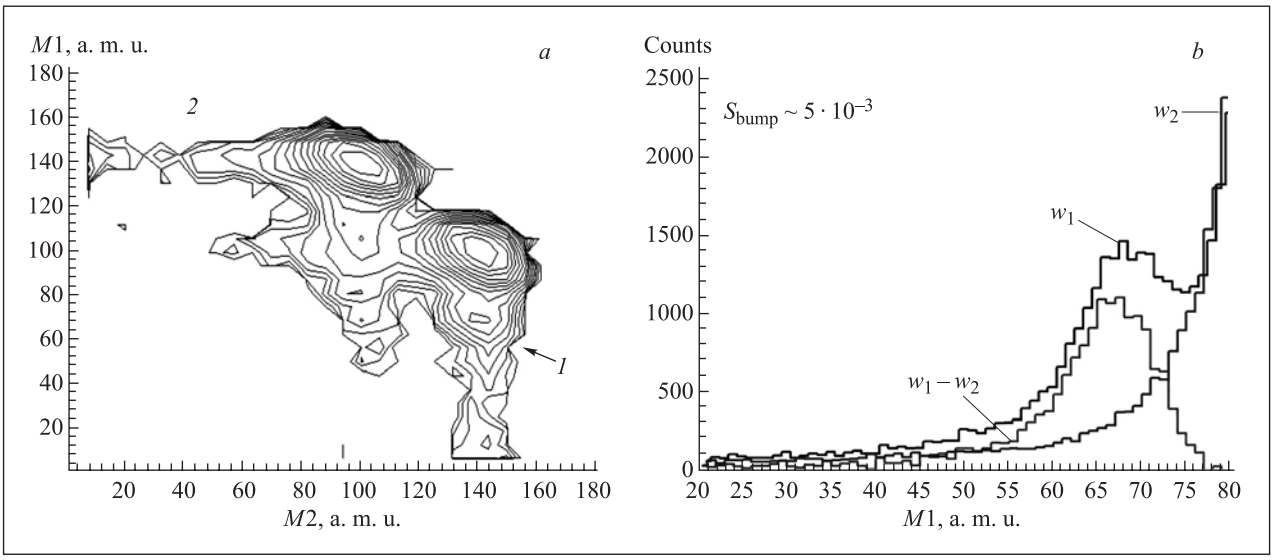

Fig. 2. *a*) Fragment mass–mass distribution (logarithmic scale) obtained for the $^{235}\mathrm{U}(n, f)$ reaction. Bump 1 under discussion is marked by the arrow; *b*) projections of the plot onto the $M1$ axis: «tail» 1 corresponds to spectrum w_1, «tail» 2 corresponds to spectrum w_2 and their difference is marked as $w_1 - w_2$

In our experiments with ^{252}Cf a specific two-dimensional bump in the fission fragments (FF) mass–mass distribution was observed. As one can see in Fig. 2, *a*, the analogous bump is clearly seen there as well. The effect manifests itself only in one of the spectrometer arms, namely, from the side of the target backing. The yield of the events, forming the bump and being of about $5 \cdot 10^{-3}$ per binary fission, was estimated after the subtraction of «tail» 2 from «tail» 1. The corresponding differential spectrum (actually the bump) is shown in Fig. 2, *b*. The bump is centered in the vicinity of masses 68–70 a.m.u associated with magic Ni isotopes.

Another manifestation of clustering was obtained as a result of special processing the fragment mass–mass distribution. Selection by the FF momentum and velocity was used. We selected events having approximately equal velocities and lying simultaneously beyond the «tails» of scattered events in the FF momentum distribution.

A specific structure in the center of the plot shown in Fig. 3 attracts one's attention. It looks like the right angle with the vertex lying at the plot diagonal in the vicinity of the point (68, 68) a.m.u. presumably linked with the magic $^{68}\mathrm{Ni}_{40}$. Using similar gating an akin

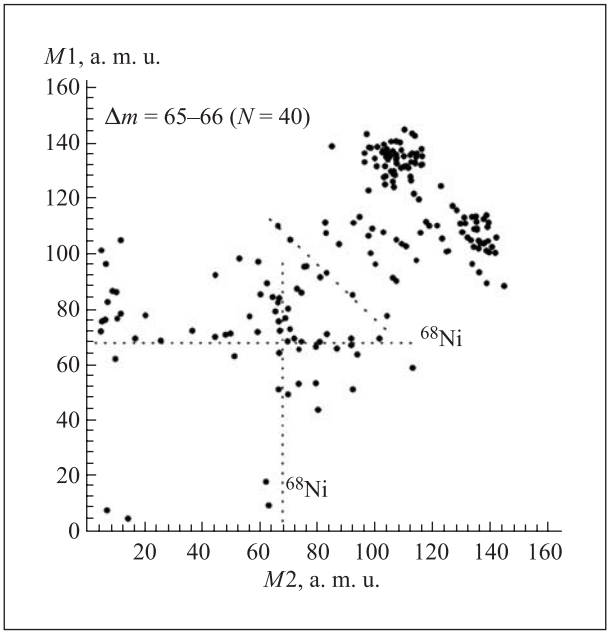

Fig. 3. Mass–mass plot for the fission events with nearly equal velocities selected beyond the «tails» of scattered fragments in the FF momentum distribution. A specific structure in the form of the right angle is clearly seen in the center of the plot. The vertex of the angle is located in the point (68, 68) presumably linked with the magic ^{68}Ni isotope

structure (rectangle) was revealed by us earlier in the mass–mass distribution of the fragments from spontaneous fission of the ^{252}Cf nucleus. Some points in the plot are likely to lie on the line $M1 + M2 = \text{const}$. The corresponding «missing fragment» is also linked with the known neutron subshell $N = 40$.

The presented results generally confirm our previous results obtained earlier for different fissioning systems [8, 9].

High-Resolution Beam-Line ACCULINNA

Recent data obtained for the spectrum of ^{9}He states [10] imply the revision of predictions for ^{10}He. Especially intriguing is the question of a $(2s)^2$ contribution into the ^{10}He low lying continuum. In order to study the structure of ^{10}He, the two-neutron transfer reaction ^{3}H(^{8}He, ^{10}He)p was investigated. The ^{3}H(^{6}He, ^{8}He)p reaction was also studied in this work, bearing in mind that the yields obtained for the known ^{8}He states populated in the similar reaction will give a reference point about the cross section value anticipated for the ^{3}H(^{8}He, ^{10}He)p reaction. Complete kinematical measurements were performed in a way similar to that used earlier in the study of the ^{5}H system. With this in view, protons emitted back from the tritium gas target in the lab system were detected in coincidence with ^{8}He(^{6}He) nuclei and neutrons originating from the ^{10}He(^{8}He) decay. Considering the lab system, these decay products were found in a rather narrow angular cone aligned with the beam axis. The observation of $p - {}^{8}$He coincidences was a sign for the ^{8}He ground state (g.s.) formation in the ^{3}H(^{6}He, ^{8}He)p reaction.

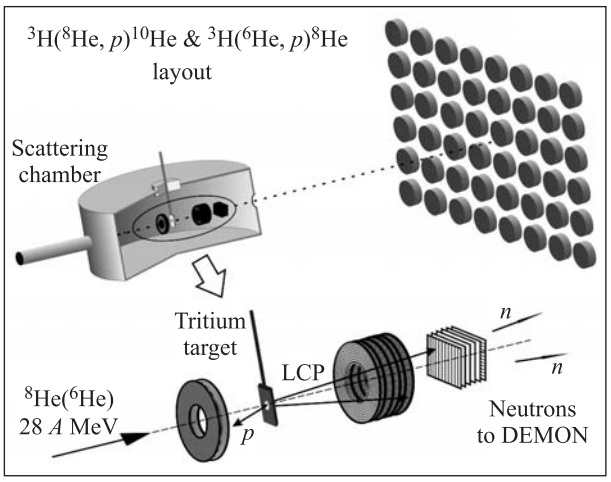

Fig. 4. Experimental setup

The experimental setup is shown in Fig. 4. A cryogenic tritium gas target containing $3{\cdot}10^{20}$ tritium atoms/cm^2 was bombarded with the 25 A MeV secondary beams of ^{8}He and ^{6}He nuclei delivered with the intensities of about $1 \cdot 10^4$ s^{-1} and $2 \cdot 10^5$ s^{-1}, respectively, from the ACCULINNA separator. A telescope composed of two highly granulated annular strip Si detectors installed at a distance of 100 mm from the target served for the detection of protons emitted within an angular range of 172 to 153 deg to the backward direction from the target. A forward, zero-angle telescope installed at a distance of 350 mm from the target measured the X and Y coordinates and accomplished the «ΔE vs E» identification of the ^{8}He(^{6}He) nuclei. Neutrons originating from the decay of ^{10}He(^{8}He) nuclei were detected by an array of 48 scintillation modules of the European time-of-flight neutron spectrometer DEMON.

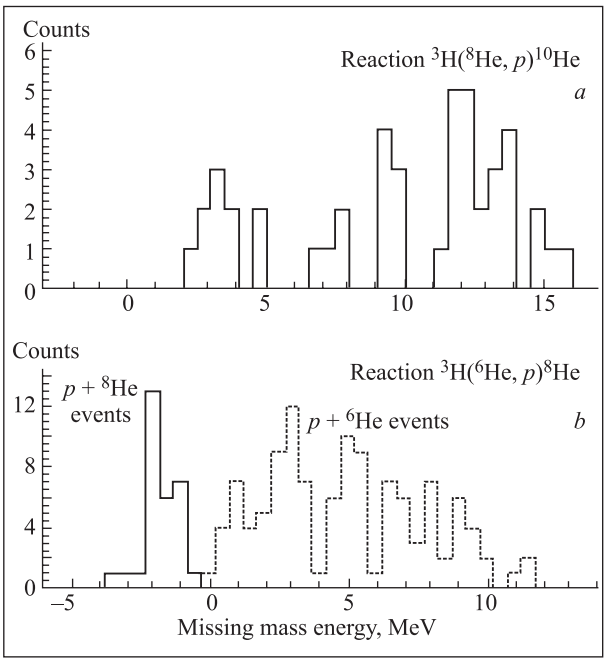

Fig. 5. Missing mass spectra obtained for the ^{10}He (a) and ^{8}He (b) nuclei. The energy scales are presented in reference to the thresholds against the $^{10}\text{He} \to {}^{8}\text{He} + n + n$ and $^{8}\text{He} \to {}^{6}\text{He} + n + n$ decays

The ^{10}He and ^{8}He missing mass spectra were for the first time studied using the ^{3}H(^{8}He, p)^{10}He and ^{3}H(^{6}He, p)^{8}He reactions. The obtained spectra are shown in Fig. 5. The ^{10}He spectrum extends from the decay threshold in $^{8}\text{He} + n + n$ to 16 MeV and altogether contains 44 events. It is noteworthy that this spectrum does not show any event lying between zero and 2 MeV, assuming that one detected event corresponds to the estimated cross section of 16 μb/sr for the ^{3}H(^{8}He, p)^{10}He reaction. The achieved low cross section limit leads one to a conclusion about the lack of a narrow ^{10}He resonance in this energy region. At the same time a well isolated group of 10 events is found between 2 and 5 MeV showing a maximum at about 3 MeV in the measured ^{10}He spectrum. Note that four of these 10 events were detected in the triple

$p - {}^8\mathrm{He} - n$ coincidence. This makes one sure that there is no background and enables one to conclude that the whole group belongs to the g.s. resonance of ^{10}He. It is worthwhile to notice that the $p - {}^8$He correlations obtained for these 10 events show a pronounced tendency to a strong final state interaction between the two neutrons emitted in the ^{10}He decay.

In the $^6\mathrm{He} + t$ experiment the population of ^{8}He g.s. was measured by the $^8\mathrm{He} + p$ coincidence (see Fig. 5, *b*). The cross section was found to be ~ 200 μb/sr. A preliminary spectrum obtained for the excited states of ^{8}He is also shown in Fig. 5. One can see that there is a sharp rise in the spectrum structure just above the $2 - n$ separation energy threshold, which is equal to 2.14 MeV for ^{8}He. If this finding is confirmed by a subsequent analysis including that of the decay properties, such a structure could be considered as a candidate for the 1^- soft dipole resonance not reported earlier for this nucleus.

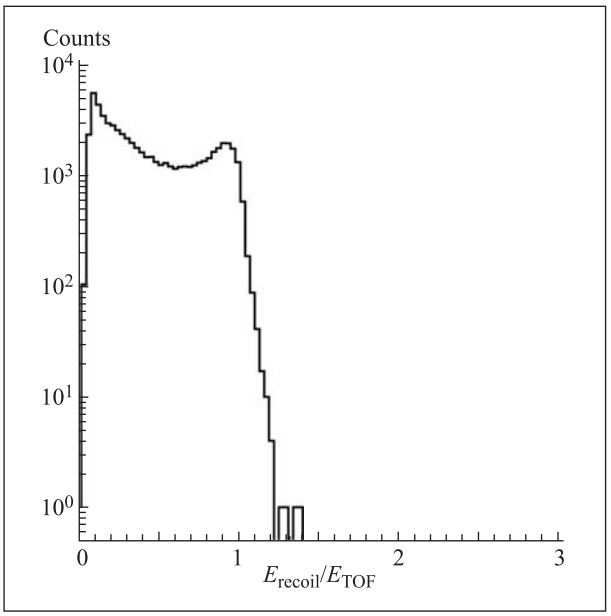

Fig. 6. Distribution in $E_{\mathrm{recoil}}/E_{\mathrm{TOF}}$ units obtained for recoiled proton events detected in the DEMON modules. The kinematics limit for a single neutron is equal to 1 assuming the ideal resolution for the measured E_{recoil}

The abundant yield obtained in the $^8\mathrm{He} + t$ experiment for α-neutron coincidence events was analyzed with the view of the search for a «heavy» («bound») tetraneutron. Figure 6 shows the coincident energy spectrum of recoiled protons in DEMON in terms of the neutron TOF. The recoiled protons with energies above the kinematics limit of a single neutron were not observed.

Reactions Induced by Stable and Radioactive Ion Beams of Light Elements

In 2007, the investigations of the energy dependences of reactions induced by the ^{6}He beam from the accelerator complex DRIBs were continued. Excitation functions were measured for fusion reactions followed by neutron evaporation, as well as for stripping and pickup reactions on a ^{197}Au target. The results were compared with similar data obtained with ^{4}He beams at the FLNR U200 cyclotron. In addition to the confirmation of the fusion enhancement for near-Coulomb barrier energies for the ^{6}He beam, a considerable cross section was observed for the one-neutron transfer reaction leading to the formation of ^{198}Au at energies 10 MeV lower than the Coulomb barrier — deeply sub-barrier transfer reaction. This observation is similar to the behaviour of (d, p)-reactions, where below the barrier a significant increase in the reaction cross section is observed (the so-called Oppenheimer–Phillips resonance due to the polarization of the weakly bound deuteron). In the ^{6}He-induced reaction, this effect can be stronger because of the smaller neutron binding energy in ^{6}He compared to that for the deuteron and the larger repulsive forces of the α-particle compared to the proton.

The excitation functions for the one-neutron transfer in the interaction of ^{6}He with ^{197}Au are presented in Fig. 7, *a*. It can be seen that the transfer of one neutron from ^{6}He to ^{197}Au is characterized by a large cross section [11]. The data obtained with the ^{6}He beam strongly differ from the results with the ^{4}He beam, whereas they show a similar behaviour as the excitation functions obtained with a deuteron beam (see Fig. 7, *b*).

Using the ^{6}He beam it was possible to measure the isomeric ratios for the products of the fusion reaction (^{196,198}Tl) and for the transfer reaction (^{196,198}Au), see Ref. [12]. It was found that the isomeric ratios for the fusion reactions followed by the evaporation of 5 and 7 neutrons exceeded by 1–3 orders of magnitude the ratios obtained for neutron transfer products. In the case of transfer reactions, the isomeric ratios for ^{196}Au and ^{198}Au show different incident energy dependence and differ in absolute value: in the case of neutron removal from ^{197}Au the isomeric ratios are higher than for the transfer of a neutron to ^{197}Au. The obtained results are important for the understanding of the reaction mechanism when weakly-bound exotic nuclei are involved, and also for astrophysics.

Experiments were also performed at the FLNR laser spectrometer. The hyperfine magnetic anomaly (HMA), connected with the radius of the valence neutron distribution, was measured for the first time in the chain including Eu-isotopes. An unusually large HMA ($> 5\%$) was observed in the isotopic pairs ^{151,152}Eu and ^{152,153}Eu. For the $^{151-154}$Eu-isotopic chain a correlation was found between the charge radii and the HMA. These results reveal the feasibility of such investigations for the determination of the hyperfine magnetic anomaly in the isotopic chain $^{150-155}$Eu and for the development of theoretical models.

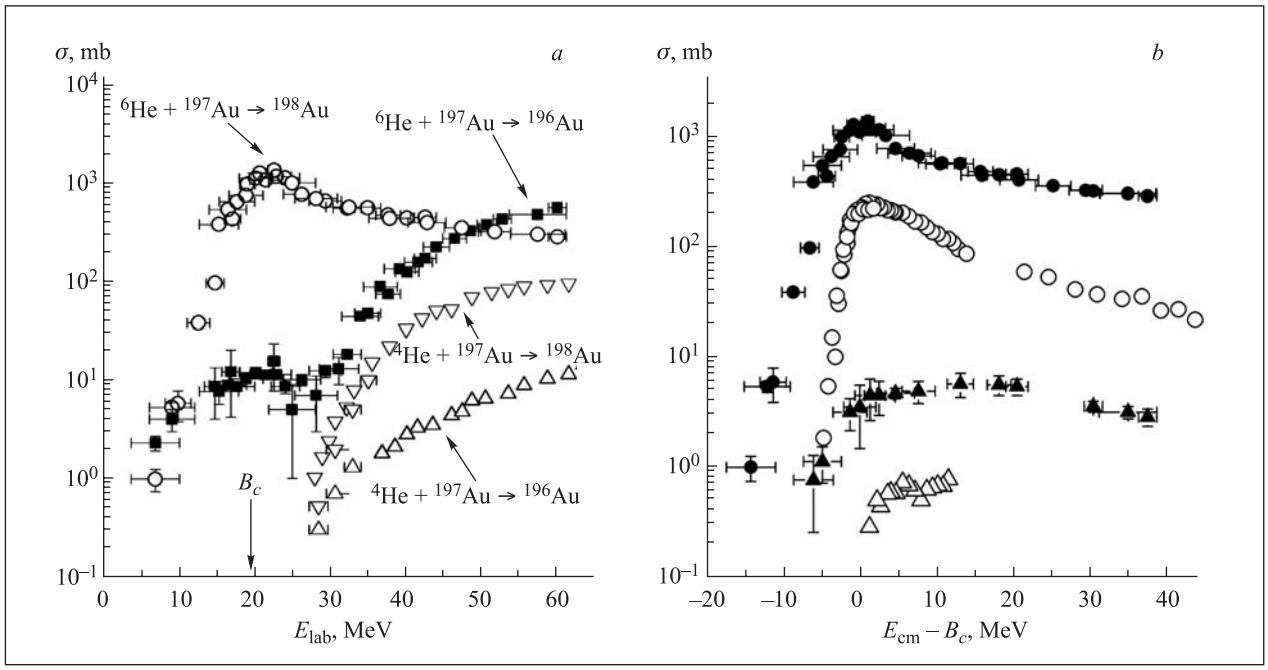

Fig. 7. *a*) Excitation functions, obtained with the ^{6}He beam, for transfer of one neutron to ^{197}Au (○) and of the one-neutron stripping (■) from ^{197}Au. The results with the ^{4}He beam — (▽) and (△) — are given for comparison; *b*) excitation functions for the production of ^{198}Au, obtained with the ^{6}He beam (black symbols) and with a deuteron beam (open symbols): circles and triangles denote the formation of the ground and isomeric states, respectively

Theoretical and Computational Physics

A multidimensional potential energy surface was derived on the basis of an extended version of the two-center shell model. It depends on several collective degrees of freedom and allows one to perform a unified analysis of deep-inelastic scattering, fusion, and fission processes.

The dynamics of heavy-ion low-energy collisions was studied within a realistic model based on multidimensional Langevin equations [13, 14]. Interplay of strongly coupled deep inelastic scattering, quasi-fission and fusion–fission processes was discussed. Collisions of very heavy nuclei (^{238}U + ^{238}U, ^{232}Th + ^{250}Cf and ^{238}U + ^{248}Cm) were investigated as an alternative way for the production of superheavy elements with the increasing neutron number. Large charge and mass transfers were found in these reactions due to the inverse (anti-symmetrizing) quasi-fission process leading to the formation of surviving superheavy long-lived neutron-rich nuclei. In many events the lifetime of the composite giant system consisting of two touching nuclei turned out to be rather long ($\sim 10^{-20}$ s) and sufficient for observing the line structure in spontaneous positron emission from superstrong electric fields which is a fundamental QED process.

The near-barrier fusion of neutron-rich nuclei was studied within the semiempirical channel coupling model for intermediate neutron rearrangement and within the time-dependent three-body Schrödinger equation [15]. The possibility of neutron transfer with positive Q values considerably increases the barrier penetrability. A huge enhancement in the deep subbarrier fusion probability was found for light neutron-rich weakly bound nuclei (such as ^{6}He). This may be quite important for astrophysical primordial and supernova nucleosynthesis.

A dynamical approach to the treatment of fission fragment angular distribution was developed. The approach is based on three-dimensional Langevin dynamics for shape collective coordinates joined with the Monte-Carlo algorithm for the degree of freedom associated with the projection K of the total angular momentum of the fissioning system on the symmetry axis. The relaxation time of the tilting mode τK was estimated. From fits to experimental data on the fission fragment angular distribution of heavy fissioning compound systems, the K equilibration time was deduced to be $\sim 4 \cdot 10^{-21}$ s for temperatures of $\sim 1{-}2$ MeV.

The possibility of synthesizing a doubly magic superheavy nucleus $^{298}114_{184}$ was investigated on the basis of fluctuation-dissipation dynamics [16]. In order to synthesize this nucleus, we must generate more neutron-rich compound nuclei because of the neutron emissions from excited compound nuclei. The compound nucleus $^{304}114$ has two advantages in achieving a high survival probability. Firstly, because of small neutron separation energy and rapid cooling, the shell correction energy recovers quickly. Secondly, owing to neutron emissions, the neutron number of the nucleus approaches that of the double closed shell and the nucleus obtains a large fission barrier. Because of these two effects, the survival probability of

$^{304}114$ does not decrease until the excitation energy $E^* = 50$ MeV. These properties lead to a rather high evaporation residue cross section.

A projection operator method was applied to the calculation of a generalized optical potential for elastic scattering induced by light nuclei taking into account the projectile breakup channels. A model proposed in previous papers was extended in order to avoid the simplifications used earlier. The model was used to describe elastic scattering of two and three cluster projectiles by heavy-ion targets at intermediate energies. In order to test the ability of the approach, elastic scattering of the deuteron was analyzed with the help of a generalized optical potential. The results were compared with the experimental data. The calculated cross sections agree well with the data. Some aspects omitted before were discussed. In particular, the role of non-physical bound states in the projectile-target system was studied. It was found to be important in deuteron elastic scattering by light nuclei. Within the approach the optical potentials of the ^{6}He (40 MeV/u) + ^{12}C reaction were calculated, assuming that ^{6}He was a two-cluster ($\alpha + {}^2n$) or three-cluster ($\alpha + n + n$) system. It was found that the optical potential turned out to be narrower within the three-cluster model than that in the case of the two-cluster approximation.

The knowledge base on low-energy nuclear physics «Nuclear Reactions Video» allocated at the website http://nrv.jinr.ru/nrv was significantly extended and improved. (i) Computational codes for calculating the driving potential energy (folding, proximity, liquid-drop and extended two-center shell models) of deformed and arbitrary oriented nuclei were included into the knowledge base. A web dialog for this model and Java applets for drawing and downloading the calculated multidimensional potential energy surfaces were written. (ii) A new code was added to the «Nuclear Models» section, providing a possibility of calculating single-particle energies and wave-functions (neutron or proton) for deformed nuclear systems proceeding from the Woods–Saxon mean field potential. (iii) Digital databases on the fusion reactions and yields of evaporation residues were filled in with several hundred experimental cross sections. All the resources of the knowledge base are available on-line via standard web browsers using CGI technology and Java applets.

Nanotechnologies and Radiation Modification of Materials

In 2007, a number of methods were developed:

- methods for the fabrication of single metal nanowires in conventional track membranes;
- methods for the fabrication of full-length copper nanowire samples for the studies using atomic force microscope;
- methods for the galvanic fabrication of monocrystal copper nanowires.

The studies of silicon samples doped by hydrogen and irradiated with Bi (710 MeV) and Kr (85 and 250 MeV) ions were performed with the use of optical and electron microscopy and recoil spectroscopy. They allowed us to find out a new experimental fact about hydrogen release from the samples.

The study of magnetic properties of nickel nanowires (30 nm) was carried out. The effect of transition from a ferromagnetic state into a diamagnetic one was found at temperatures of about 50–60 K.

The study of surface sputtering processes in a number of model and constructive reactor materials depending on the ionizing energy loss of heavy-ions and damage dose level was continued. Studies of nanoscale structural defects on the surface of single crystalline Al_2O_3, ZrO_2:Y and $MgAl_2O_4$, irradiated with krypton, xenon and bismuth ions with the fission fragment energy are underway using atomic force microscopy. The systematization of experimental data on geometrical parameters of defects formed by single heavy-ions as a function of electronic stopping power was continued.

In-situ piezospectroscopic studies of mechanical stress in radiation-resistant oxides under the irradiation with 1 MeV/amu heavy-ions in dependence on the ionization density, ion fluence and irradiation temperature were continued. The analysis and systematization of experimental data are underway.

The first experiments aimed at the study of radiation hardness of nanostructured semiconductors (GaN) against high-energy heavy-ion irradiation were carried out.

The main results were published in [17–21].

Track Membranes and Modification of Polymers

Development of production methods of asymmetric micro- and nanopores using chemical treatment of heavy-ion irradiated polymers was continued in 2007. Methods allowing control over the pore profile were suggested. Electrochemical properties of asymmetric nanoporous membranes were investigated. It was shown that geometrical asymmetry leads to diode-like properties. Effect of electrical current rectification in asymmetric nanopores filled with an electrolyte was investigated in dependence on the electrolyte concentration, pore size and the degree of geometrical asymmetry [22]. The obtained results were published in «Nanotechnology». In collaboration with the Institute of Spectroscopy of RAN (Troitsk) and in the framework of RFBR grant No. 06-08-01299a, experiments on atom beam lithography with the use of asymmetric track-etched nanopores are in progress.

The first phases of the work on the development of track membranes with improved permeability and improved chemical stability were completed. The work entitled «Creation of the Scientific Basis for the Production Technology of Track Membranes from Polyethylene Terephthalate and Polyethylene Naphthalate.

Upgrading Irradiation and Chemical Etching Setups» was financed by the Federal target program «Investigation and Development in Priority Directions of Development of Scientific and Technological Russian Complex for 2007–2012» (action 1.3 of the Program — II stage) in the framework of agreement No. 58/801/19-07 between the Shubnikov Institute of Crystallography of RAS and the Joint Institute for Nuclear Research.

In collaboration with the Institute of Acoustics (Madrid, Spain), experiments on the propagation of ultrasonic waves of different frequencies through track membranes were carried out. It was shown that an ultrasonic wave going through a membrane was split into two components. One component is a wave propagating through membrane matrix, while the other one is propagating through air filling the pores. Phase and magnitude of the second component can be measured and used for the estimation of membrane properties such as porosity and pore diameter [23].

The structure and electrotransport properties of polyethyleneterephthalate track membranes modified by plasma of thiophene were investigated. The influence of the degree of oxidation by iodine or UV-irradiation of the polymeric layer formed by plasma on the membrane characteristics was studied. It was found that deposition of the polymeric layer on the surface of the track membranes with the help of polymerization of the thiophene vapors in plasma leads to the formation of composite membranes possessing the asymmetry of conductivity (rectification effect) in a potassium chloride solution. It is caused by the presence in the modified membranes of two layers with antipolar conductivity. It was shown that doping the polymer layer formed in plasma by iodine or effect of the UV-irradiation caused a change in the density of a positive charge on its macromolecules and thus led to a change in the rectification effect.

A procedure of template synthesis of micro- and nanostructural materials (nanowires, nanotubules as well as nanomembranes with a selective layer) on the basis of copolymers from styrene, butylmethacrylate and 4-aminostyrene was developed. Similar polymeric compositions can be used as matrices in nonlinear optics to create electronic and optical nanodevices. As a template, poly(ethylene terephthalate) track membranes with the effective pore diameter from 0.15 to 0.55 μm were used. The laws of formation of these materials and their structural properties were investigated. To produce the polymeric nanomaterials a flushing method was used. It was shown that varying the parameters of the process of deposition of copolymers on the track membrane surface provided a way for producing a big assortment of composite nanomembranes with a selective layer as well as nanowires and nanotubules with a wide spectrum of characteristics.

Ultra Pure Radioisotopes and Radio Analytical Research

Production of Radioisotopes

1. Ultrapure (radionuclide-pure) preparations of radioactive carrier-free isotopes ^{88}Zr, ^{92m}Nb,^{99}Mo(^{99m}Tc), ^{97}Ru, ^{109}Cd, ^{111}In,^{175}Hf, ^{177}Ta, ^{178}W(^{178}Ta), ^{186}Re, ^{188}Re, ^{211}At, ^{237}U, ^{236,237}Pu, etc., were produced.

2. New methods of separation and concentration of radioisotopes (selective nuclear reactions, recoil, radiochemical separation) were developed.

3. New methods of the ^{237}U and ^{238}U separation with the factor of enrichment of 10^6 were developed.

4. The reaction $^{226}\mathrm{Ra}\,(\gamma, n)\,^{225}\mathrm{Ra} \rightarrow {}^{225}\mathrm{Ac}$ was studied with the view of the ^{225}Ac production for the purposes of biomedical research.

Radioanalytical Studies

1. X-ray fluorescence, gamma and neutron-activation analysis of soil and moss samples was carried out, as well as the analysis of metallurgical pollution in soil samples from the vicinities of a lead-zinc plant in Bulgaria.

2. X-ray fluorescence, gamma and neutron-activation analysis of sediments from Mongolian lakes (Lake Khar nuur in Khentii and Lake Ikh tsaidam) used in medicine was carried out.

State of Radioactive Elements in Water Environments

1. Results on the determination of K_d (factor of distribution) for U, Mo, Eu, Ba, Ce, Mn and Y in the system soil–solution in a pH range of 1–7 were analyzed (Bulgaria).

2. Study of the distribution of ^{237}U in the humus acid/solution system was continued (Manchester University, England).

Physics and Heavy-Ion Accelerator Techniques

U400 Cyclotron. The major part of the U400 operating time was devoted to the acceleration of high-intensity beams of ^{48}Ca ions which are extensively used in the synthesis of a number of new isotopes of superheavy elements. Since recently much work has been done in view of the preparation of the U400 cyclotron for complete modernization. It is planned to:

1. Increase beam intensities of ions with masses $A \sim 50$ and energies ~ 6 MeV/A up to the level of 4 pμA (20 eμA for $^{48}\mathrm{Ca}^{5+}$).

2. Provide the variation of the beam energy by a factor of 5.

3. Reduce the energy spread of the beam to the level of 10^{-3}.

4. Guarantee the beam emittance on the target of no more than 10π mm $\cdot$ mrad.

5. Reduce the average magnetic field from the 2 T level to a lower value.

6. Provide easy and fast variation of the magnetic field in a range from 0.8 to 1.8 T.

7. Replace the obsolete equipment by new modern systems.

The U400 cyclotron will be upgraded after the modernization of the U400M cyclotron and installation of a new experimental equipment (the Separator MASHA and Gas Filled Separator GFS) in the experimental area of the U400M cyclotron.

U400M Cyclotron. A new axial injection line for the U400M cyclotron was designed, fabricated and tested and a new ECR ion source was installed. In 2008, we plan to install the second ion source — the superconducting DECRIS-SC2. The low-energy beam line ($3 \div 9$ MeV/A) was assembled. It is expected that the modified U400M cyclotron will start its operation in the autumn of 2007.

Within the framework of the DRIBS (Dubna Radioactive Ion Beam) Project the U400 and U400M cyclotrons will be used for the acceleration of ^{6}He and ^{8}He radioactive beams.

IC-100 Cyclotron for Applied Research. The IC-100 cyclotron for applied research worked successfully for the irradiation of polymer films used in the industrial production of Track Membranes (TM). Beams of Kr^{15+} and Xe^{23+} heavy ions were accelerated and delivered to the target for the TM fabrication. The beam intensities as high as 2.5 eμA for Kr ions and 1.3 eμA for Xe ions were achieved. Heavy-ions of Ar, Fe, I and W were also accelerated at the IC-100 cyclotron for the purposes of scientific and applied research activities.

Development of the ECR Ion Sources. The development of new improved ion sources using the electron cyclotron resonance (ECR) is stimulated at the Flerov Laboratory of Nuclear Reactions by demands of upgrading the accelerator complex based on U400, U400M and CI-100 cyclotrons. New ECR sources are also necessary for the production of secondary radioactive ion beams.

Over the past 15 years several types of ECR ion sources of the DECRIS (Dubna Electron Cyclotron Resonance Ion Source) family were developed at the FLNR (JINR). In the traditional version of the source the formation of the axial magnetic field (1–1.3 T in the maximum of the distribution) is performed with the use of water cooled copper coils. The radial magnetic field ($\sim$ 1 T at the discharge chamber wall) is created by a permanent magnet (NdFeB) hexapole. For the plasma heating a microwave generator of the frequency of 14 GHz is used.

In the new generation of ECR ion sources DECRIS-SC a superconducting magnet system is used for the axial magnetic field formation (the maximum in the distribution at 2 and 3 T). For the solenoid coils cooling a compact refrigerator of the Gifford–McMahon type is used. The magnet system allows one to use the microwave frequency in a range of 14–28 GHz for plasma heating. The design and production of compact versions of the ion sources DECRIS-SC2 and DECRIS-SC3 with the plasma heating frequencies of 14 and 18 GHz, correspondingly, are underway.

A project of an ECR ion source with the axial and radial magnetic field formation by the superconducting windings is planned.

For the production of stable and radioactive single charged ions the ion sources operating at the frequency of 2.45 GHz were developed at the FLNR. The magnet system of the ion sources of this type consists of a set of permanent magnet (NdFeB) rings. These ion sources are capable of producing beams of single charged ions of gases with the efficiency of about 80% for Kr, Xe, and about 15% for He. The developed sources are in operation at the DRIBs (Dubna Radioactive Ion Beams) facility and are used for the production of $^{6}He^{+}$ and $^{8}He^{+}$ ions, and at the mass-spectrometer MASHA (Mass Analyzer of Super-Heavy Atoms).

REFERENCES

1. *Stoyer N. J. et al.* // Nucl. Phys. A. 2007. V. 787. P. 388–395.
2. *Oganessian Yu. Ts. et al.* // Phys. Rev. C. 2007. V. 76. P. 011601.
3. *Eichler R. et al.* // Nature. 2007. V. 447. P. 72.
4. *Knyazheva G. N. et al.* // Phys. Rev. C. 2007. V. 75. P. 05562813.
5. *Hofmann S. et al.* // Eur. Phys. J. A. 2007. V. 32. P. 251–260.
6. *Lopez-Martens A. et al.* // Ibid. P. 245–250.
7. *Hofmann S. et al.* // Intern. J. Mod. Phys. E. 2007. V. 16, No. 4. P. 937–947.
8. *Zherebchevsky V. et al.* // Phys. Lett. B. 2007. V. 646. P. 12–18.
9. *Zherebchevsky V. et al.* // Pis'ma v ZhETF. 2007. V. 85, No. 3. P. 168–173.
10. *Golovkov M. S. et al.* // Phys. Rev. C. 2007. V. 76. P. 021605(R).
11. *Penionzhkevich Yu. E. et al.* // Eur. Phys. J. A. 2007. V. 31. P. 185.
12. *Kulko A. A. et al.* // Phys. G: Nucl. Part. Phys. 2007. V. 34.
13. *Zagrebaev V. I., Greiner W.* // Nucl. Phys. A. 2007. V. 787. P. 363.
14. *Greiner W., Zagrebaev V. I.* // Intern. J. Mod. Phys. D. 2007. V. 16. P. 141–153.
15. *Zagrebaev V. I. et al.* // Phys. Rev. C. 2007. V. 75. P. 035809.
16. *Aritomo Y.* // Ibid. P. 024602.
17. *Reutov V. F., Dmitriev S. N.* // Pis'ma v ZhTF. 2007. V. 33, Issue 5. P. 41–45.
18. *Reutov V. F., Miklyaev M. F.* // Instr. Exp. Techn. 2007. No. 3. P. 140–143 (in Russian).
19. *Reutov V. F. et al.* // Idid. P. 144–147.
20. *Ursaki V. V. et al.* // Appl. Phys. Lett. 2007. V. 90. P. 161908-1–161908-3.
21. *Kuzmin V.* // Nucl. Instr. Meth. B. 2007. V. 256. P. 105–108.
22. *Apel P. Yu. et al.* // Nanotechnology. 2007. V. 18. P. 305302.
23. *Gómez Álvarez-Arenas T. E. et al.* // J. Membr. Sci. 2007. V. 301. P. 210–220.